Applied Thermal Engineering 111 (2017) 317–324

Contents lists available at ScienceDirect

Applied Thermal Engineering

journal homepage: www.elsevier.com/locate/apthermeng

Research Paper

Effect of internal heat leakage on the performance of a high pressure ratio centrifugal compressor

S. Mostafa Moosania, Xinqian Zheng *

Turbomachinery Laboratory, State Key Laboratory of Automotive Safety and Energy, Tsinghua University, Beijing 100084, China

HIGHLIGHTS

- The effects of internal heat leakage intensifies with increasing the pressure ratio.
- Internal heat leakage should be considered at the pressure ratio higher than 5.
- Internal heat leakage inside the impeller reduces the impeller maximum temperature.
- Heat leakage inside the casing degrades the compressor performance.

ARTICLE INFO

Article history:
Received 6 April 2016
Revised 4 September 2016
Accepted 7 September 2016
Available online 16 September 2016

Keywords:
Centrifugal compressor
High pressure ratio
Internal heat leakage
Conjugate Heat Transfer (CHT)

ABSTRACT

Centrifugal compressors are widely used in compact gas turbines in industrial and military applications where a high pressure ratio in small size is needed. The trend in centrifugal compressor is high pressure ratios and high efficiencies. However, higher pressure ratio increases the temperature difference between upstream flow and downstream flow which leads to a heat leakage from downstream to upstream through the solid parts. This heat leakage negatively affects the performance as well as the reliability of the compressor. In this study the effect of heat leakage through solid impeller and casing on the compressor performance has been studied for different pressure ratios. The compressor performance has been calculated using a three dimensional numerical model. Conjugate Heat Transfer (CHT) method has been used to calculate the temperature in the solid parts. The results show that the internal heat leakage through both the impeller and casing reduces the efficiency by 2.5% and the total pressure ratio by about 0.83 at pressure ratio up to 11. The effect of the internal heat transfer on the compressor performance is more noticeable at pressure ratios higher than 5. Meanwhile, heat transfer inside the solid impeller alone from the hot region to the cool region reduces the maximum impeller temperature while this heat leakage has a small effect on the compressor performance. However, heat leakage inside the casing alone slightly increases the impeller temperature while it strongly affects the compressor performance.

1. Introduction

Demands for compact, efficient high pressure ratio centrifugal compressors are increasing in both commercial and military applications. Such compressors reduce the size and weight of the system. However, high rotational speed of the impeller and high Mach number of flow require a carefully designed compressor to maintain the reliability and efficiency. The main focus of recent studies about centrifugal compressors with high pressure ratio was to increase the efficiency [1–4].

Another factor that affects the compressor efficiency is the heat transfer. Usually the compressor is not adiabatic, and therefore there is heat exchange between the compressor and the surrounding. For instance, for a turbocharger installed in a car, the heat transfer from the engine and the turbine to the compressor is proved to reduce the efficiency of the compressor by about 25% on average [5]. Meanwhile, heat transfer to the compressor increases the impeller temperature which degrades its reliability. The maximum pressure ratio in which the impeller can bear will be reduced if the effect of heat transfer to the solid impeller is taken into account because the allowable ultimate stress is reduced with increased temperature [6].

Heat transfer to the outside or cooling on the other hand improves the performance and reliability of the compressor.

* Corresponding author.
E-mail address: zhengxq@tsinghua.edu.cn (X. Zheng).

http://dx.doi.org/10.1016/j.applthermaleng.2016.09.030
1359-4311/

Nomenclature

h	specific enthalpy (J/kg)
D_2	impeller diameter (mm)
F_2	blending function (–)
f_r	correction factor (–)
m	mass flow rate (kg/s)
n	rotational speed (rpm)
P	pressure (Pa)
P_k	shear production of turbulence (kg/m s^3)
P'	corrected pressure (=p + 2ρk/3)
q	heat transfer per mass flow (J/kg)
R	specific gas constant (J/kg-K)
Re	Reynolds number (ρUL/μ)
s	entropy (J/kg K)
S_m	momentum source term
S_E	energy source term
T	temperature (K)
Z	number of blades or vanes (–)
U	velocity (m/s)
u	velocity fluctuation (m/s)
y+	dimensionless wall distance (–)

Greek symbols

∇	nabla sign
μ	air viscosity (kg/m s)
λ	thermal conductivity (W/m K)
η	efficiency (%)
ρ	density (kg/m^3)
τ	shear stress (N/m^2)

Subscriptions

p	polytropic
s	isentropic
t	turbulence
0	stagnation condition
1	inlet
2	outlet
θ	tangential direction

Gwehenberger [7] found that cooling a centrifugal compressor allows the compressor pressure ratio to increase from 5.2 to 5.8. Also cooling itself can increase the pressure ratio and efficiency of the compressor by changing the thermodynamical path of the compression process [8].

There is a temperature increase in compressors resulted by compression of the flow. The resulted temperature difference produces a heat flux in the solid parts from high temperature regions located in downstream to low temperature regions in upstream. This heat leakage is more noticeable in centrifugal compressors due to small distance between downstream and upstream. The heat leakage through the solid parts affects the efficiency as well as the reliability of the compressor. Gu [9] studied the effect of internal heat transfer as well as heat transfer to a centrifugal compressor through different parts. They reported that for a centrifugal compressor with pressure ratio of 2.8, internal heat leakage reduces the compressor efficiency by 0.85%. Their study focused on the design point and they also neglect the heat transfer in the casing in the backplate.

Based on the results obtained by Cui [10], internal heat transfer affects the compressor efficiency considerably and the amount of heat circulating through the solid parts of compressor ranges from 5% to 9% of the input energy of the impeller. This high circulation of heat transfer can have a huge effect on the flow field and performance of the compressor as well as temperature of different parts. This heat transfer is usually neglected in compressor CFD calculations, which may lead to significant errors in the results.

In this paper the effects of internal heat leakage on the performance and reliability of a high pressure ratio centrifugal compressor have been studied using a three dimensional RANS model. The heat leakage originated in the compressor casing or the solid impeller, from hot downstream to the cool upstream. The heat leakage through both routes together and only one route was studied in different pressure ratios.

2. Numerical model

2.1. Compressor geometry

The compressor has an impeller with 9 blades and 9 splitters. The compressor parameters are shown in Table 1. Only one passage including one main blade and one splitter is modeled for calculation. Solid casing was designed according to conventional designs of high pressure ratio compressors in gas turbines (Fig. 1). The solid parts are made by aluminum with thermal con-

Table 1
Compressor parameters.

Parameters	Value and units
n, (Rotational speed)	100,000 (rpm)
m, (Mass flow rate)	0.71 (kg/s)
Z, (Blades number)	9 + 9 (–)
D_2, (Impeller outlet diameter)	120 (mm)
Tip clearance	0.5 (mm)
Air gap width	1 (mm)
Blade inlet angle	60 (°)
Back sweep	40 (°)
Re tip	4.96e6

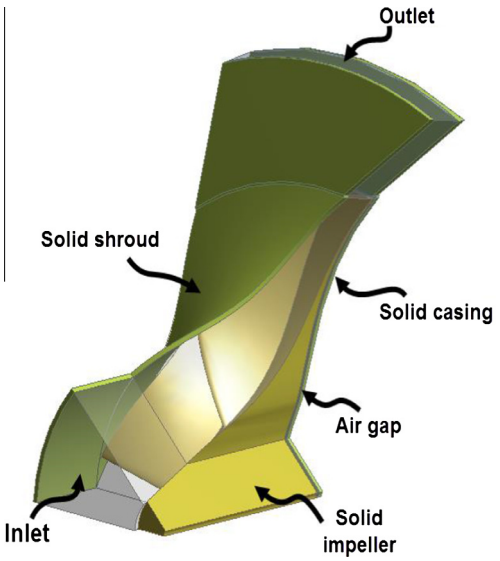

Fig. 1. One compressor sector and the solid parts.

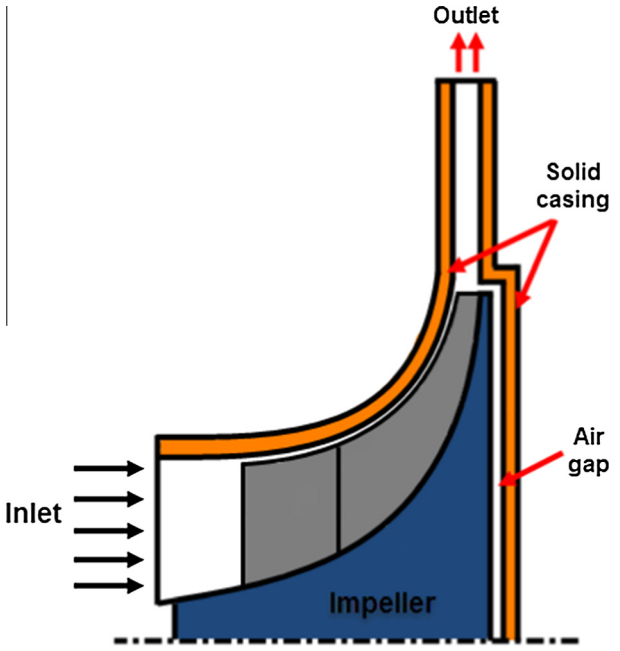

Fig. 2. Centrifugal compressor with the solid casing.

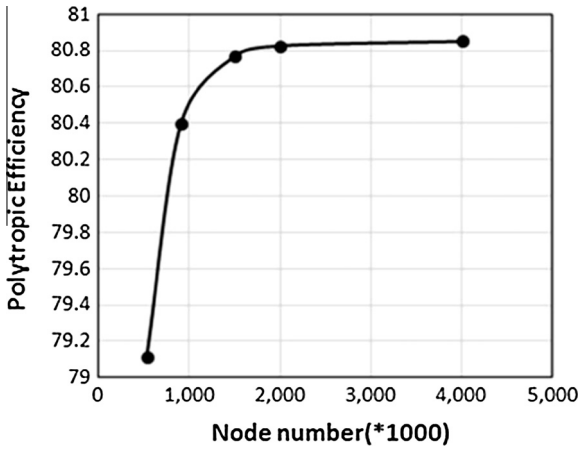

Fig. 3. Polytropic efficiency variation with different size meshes.

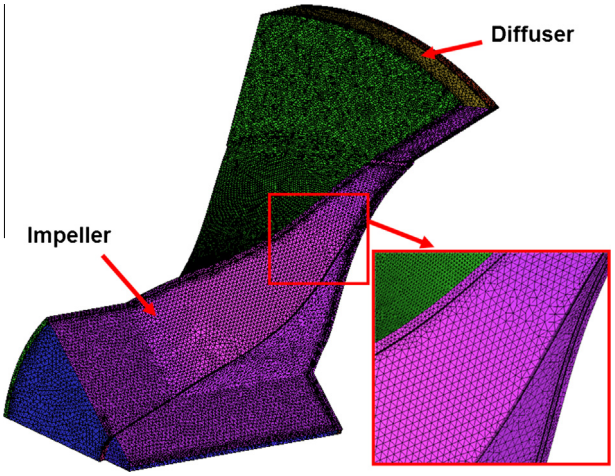

Fig. 4. Grid generated for the simulation.

ductivity of 202 W/m^2 K. The solid parts and the air flow are shown in Fig. 2.

2.2. Mesh generation

A refined grid was created for the rotating impeller as well as the stationary solid parts and the diffuser. The grid was generated together for the solid and fluid domains to have the same nodes on the fluid-solid interfaces. This increases the accuracy of the fluid-solid interaction calculation [11]. All the grids had 10 prism layers near the walls with $y^+ < 1$. After a grid independence check (Fig. 3), the final grid consisted of about 2 million nodes as shown in Fig. 4.

2.3. Boundary conditions

The inlet conditions were a total pressure of 100 kPa and a total temperature of 298.15 K with a moderate turbulence intensity of 5% and flow in the axial direction. The outlet static pressure of the same value as the inlet total pressure was used to find the choke point. Then, the mass flow rate was set at the outlet to the values lower than the choked mass flow rate so as to find other operating points.

The heat transfer to the surroundings was neglected and all the surfaces exposed to the environment are assumed to be adiabatic. This assumption is reasonable because there is much more heat transfer inside the high speed compressor than the natural convection heat transfer on the outside walls. Meanwhile, this study considers the effects of heat transfer through the solid parts and the small heat transfer to the surrounding wouldn't have a very large effect on the temperature profile in the solid parts. No-slip wall boundary conditions were applied to all the walls. The high rotational speed of the impeller produces a high convection coefficient on the backplate disk. However, the heat transfer by convection is very large and the temperature difference between backplate and the impeller is very small due to this heat transfer. As a result the radiation in the casing and all other parts can be neglected.

Unsteady calculation for sure has a better result in turbomachinery application. Unfortunately, high calculation cost of URANS makes it difficult to use for a very refined grid. Thanks to different interface models solving RANS equation for unsteady turbomachinery applications is possible. As illustrated in the validation part the results are in a good agreement with the experimental data. Steady-state calculations were used by adding a rotating interface between the rotating impeller and stationary diffuser fluid domains. The staged model performs circumferential averaging of the fluxes through the interface. Steady state solutions are then obtained in each reference frame. The stage averaging in each frame on the interface creates a one-time mixing loss. This loss is equivalent to assuming that the physical mixing supplied by the relative motion between components is sufficiently large to cause any upstream velocity profile to mix out prior to entering the downstream component. The stage analysis is most appropriate when the circumferential variation of the flow is on the order of the component pitch.

2.4. Numerical methodology

The CFX commercial solver was used to solve the steady-state Reynolds Average Navier-Stokes (RANS) equations for the compressible air flow inside the compressor. The air was assumed to be an ideal gas. Although the compressor has a high outlet pressure it is far below this critical pressure. Also the air temperature increases several times more than the critical temperature due to compression process. Based on compressibility diagram ideal gas assumption still has a good prediction of air properties.

$$p = \rho RT \tag{1}$$

The flow inside a high speed compressor is fully turbulent. Thus, the SST (Shear Stress Transport) model was used for the turbulence closure in the RANS equations. This model combines the accuracy of the k-ω model for boundary layer predictions in high adverse pressure gradient flows and the stability of the k-ε model for the main flow. Therefore, the SST model balances the accuracy and stability [12]. Also, SST model has good accuracy for conjugate heat transfer calculations [13].

2.4.1. Reynolds averaged Navier Stokes equations

The flow velocity U_i, is divided into an average component, $\overline{U}_i$, and a time varying component, u_i. The averaging for the compressible flow is weighted by the density (Favre-averaging):

$$U_i = \overline{U}_i + u_i \tag{2}$$

Substituting the averaged quantities into the original transport equations results in the Reynolds averaged equations for steady-state flow given by the following:

$$\frac{\partial}{\partial x_j}(\rho U_j) = 0 \tag{3}$$

$$\frac{\partial}{\partial x_j}(\rho U_i U_j) = -\frac{\partial p'}{\partial x_i} + \frac{\partial}{\partial x_j}\left[\mu_{eff}\left(\frac{\partial U_i}{\partial x_j} + \frac{\partial U_j}{\partial x_i}\right)\right] + S_M \tag{4}$$

where p' is the corrected pressure

$$p' = p + \frac{2}{3}\rho k \tag{5}$$

k and μ_{eff} were calculated using the following:

$$k = \frac{1}{2}\overline{u_i^2} \tag{6}$$

$$\mu_{eff} = \mu + \mu_t \tag{7}$$

where μ_t is the turbulent viscosity which for the SST model with wall treatment is calculated by the following:

$$\mu_t = \frac{a_1 k/\rho}{\max(a_1\omega, SF_2)} \tag{8}$$

where k is the turbulent kinetic energy defined as the variance of the velocity fluctuations. ω is the turbulent Eddy dissipation (the rate at which the velocity fluctuations are dissipated). S is an invariant measure of the strain rate. F_2 is a blending function which is used in CFX to treat the boundary layer. F_2 is equal to 1 near the surface and becomes zero outside the boundary layer.

The values of k and ω come directly from the differential transport equations for the turbulent kinetic energy and the turbulent dissipation.

$$\frac{\partial(\rho k)}{\partial t} + \frac{\partial}{\partial x_j}(\rho U_j k) = \frac{\partial}{\partial x_j}\left[\left(\mu + \frac{\mu_t}{\sigma_k}\right)\frac{\partial k}{\partial x_j}\right] + P_k - \beta'\rho k\omega \tag{9}$$

$$\frac{\partial(\rho\omega)}{\partial t} + \frac{\partial}{\partial x_j}(\rho U_j \omega) = \frac{\partial}{\partial x_j}\left[\left(\mu + \frac{\mu_t}{\sigma_\omega}\right)\frac{\partial \omega}{\partial x_j}\right] + \alpha\frac{\omega}{k}P_k - \beta\rho\omega^2 \tag{10}$$

where the constants are as follows:

$$\alpha = 5/9$$
$$\beta = 0.075$$
$$\beta' = 0.09$$
$$\sigma_k = \sigma_\omega = 2$$

P_k is called the shear production of turbulence calculated as follows:

$$P_k = \mu_t\left(\frac{\partial U_i}{\partial x_j} + \frac{\partial U_j}{\partial x_i}\right)\frac{\partial U_i}{\partial x_j} - \frac{2}{3}\frac{\partial U_k}{\partial x_k}\left(3\mu_t\frac{\partial U_k}{\partial x_k} + \rho k\right) \tag{11}$$

The problem with the two equation turbulence models is that they are insensitive to the stream line curvature and system rotation. These effects are very important in high-speed rotating compressors. A correction factor introduced by Spalart and Shur [14], is used in CFX code to take into account the effects of streamline curvature on the turbulent kinetic energy.

$$P_k \rightarrow P_k \cdot f_r \tag{12}$$

with the correction factor f_r limited between 0 for stabilized flows and 1.25 for highly rotational flows.

The Reynolds averaged energy equation is as follows:

$$\frac{\partial}{\partial x_j}(\rho U_j h_{tot}) = \frac{\partial}{\partial x_j}\left(\lambda\frac{\partial T}{\partial x_j} - \rho\overline{u_j h}\right) + \frac{\partial}{\partial x_j}\left[U_i(\tau_{ij} - \rho\overline{u_i u_j})\right] + S_E \tag{13}$$

The unknown Reynolds stress tensor $\overline{u_i u_j}$, is calculated from the following:

$$-\rho\overline{u_i u_j} = \mu_t\left(\frac{\partial U_i}{\partial x_j} + \frac{\partial U_j}{\partial x_i}\right) - \frac{2}{3}\delta_{ij}\left(\rho k + \mu_t\frac{\partial U_k}{\partial x_k}\right) \tag{14}$$

The term $\frac{\partial}{\partial x_j}\left[U_i(\tau_{ij} - \rho\overline{u_i u_j})\right]$ is the viscous work.

2.4.2. Advection discretization method

In the beginning of the simulation, the 1st order upwind method was used for the advection terms because of its better convergence and stability. The High Resolution advection scheme in the CFX package was then used for the final results due to the false diffusion in the first order upwind method.

$$\varphi_{ip} = \varphi_{up+}\beta\nabla\varphi.\Delta\vec{r} \tag{15}$$

The High Resolution Scheme uses a special nonlinear recipe for β at each node, computed to be as close to 1 as possible without introducing new extrema. The advective flux is then evaluated using the values of β and $\nabla\varphi$ from the upwind node. The recipe for β is based on the boundedness principles used by Barth and Jesperson [15]. The choice of $\beta = 1$ leads to formally second-order-accurate discretization in space.

2.4.3. Conjugate heat transfer

The Conjugate Heat Transfer (CHT) method was used to calculate the temperatures in the solid impeller and the solid casing. The CHT method gives accurate predictions of the temperatures with low computational cost and has been valid by many authors [16,17]. The CHT method uses the same code to solve for both the solid and fluid temperatures with only the energy equation solved inside the solid body.

$$\nabla\cdot(\rho U_s h) = \nabla\cdot(\lambda\nabla T) + S_E \tag{16}$$

where h is the enthalpy, ρ is the density and λ is the thermal conductivity of the solid. U_s is the velocity of the solid.

The presented numerical method then has been validated with open literature results for a high pressure ratio compressor by Krain and Hofmann [18]. The numerical results are in a good agreement with the experimental data as illustrated in Fig. 5.

3. Results and discussion

3.1. Effect of the internal heat transfer on the pressure ratio

The predicted pressure ratios for different mass flow rates and speeds for cases with and without solid parts are shown in Fig. 6. The heat transfer through the solid parts from downstream to upstream negatively affects the compressor pressure ratio. The highest difference occurs in the lowest mass flow rate in each speed line. The values of pressure ratio for these points have been

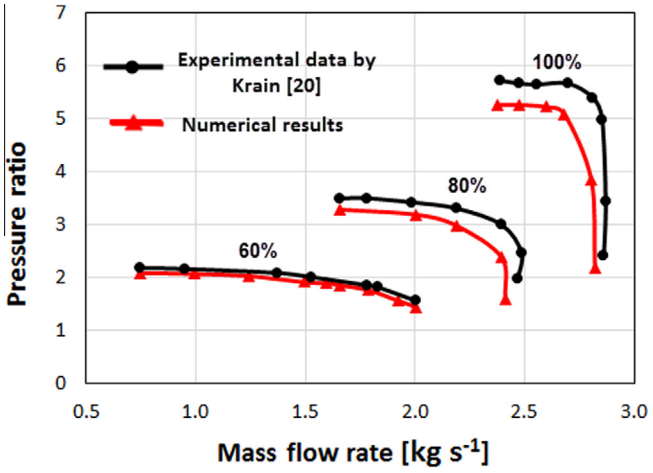

Fig. 5. Numerical validation using the experimental results obtained by Krain [18].

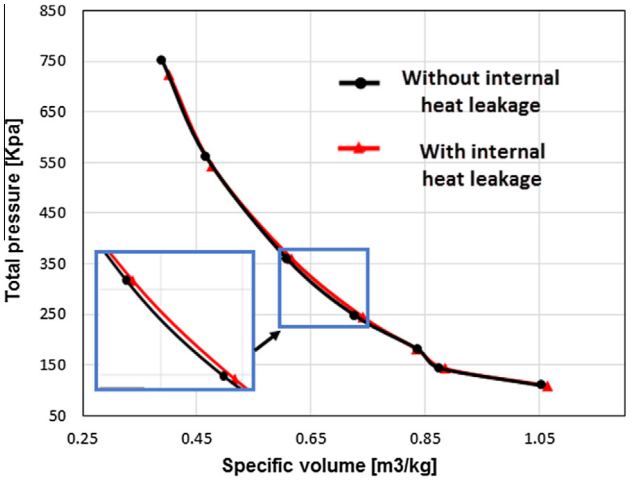

Fig. 7. P-v diagram of the compression process.

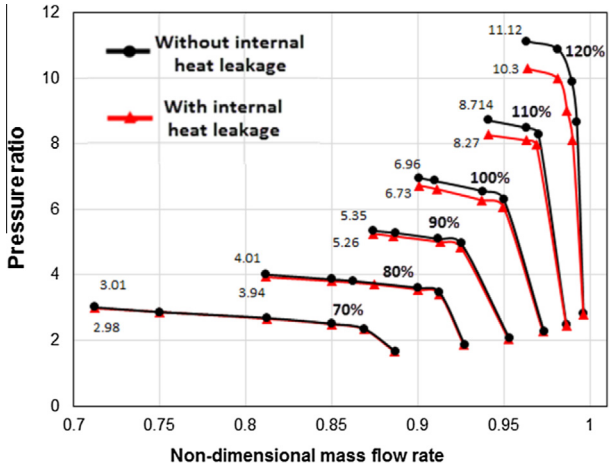

Fig. 6. Effect of the internal heat transfer on the pressure ratio.

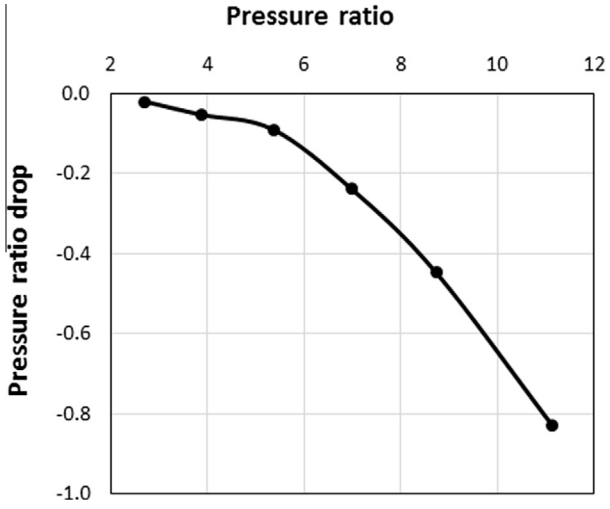

Fig. 8. Pressure ratio drop due to internal heat transfer.

illustrated on the graph. The negative effect of internal heat transfer raises with increasing the pressure ratio and rotational speed. The difference in pressure ratios is more noticeable at pressure ratios higher than 5. The pressure ratio drop is larger in higher pressure ratios because of higher temperature difference across the compressor. The effect of the internal heat transfer is small at lower pressure ratios.

The effect of the internal heat transfer on the total pressure ratio can be explained using Fig. 7. The total pressure of the flow, p_0, and the specific volume, υ, were calculated in the streamwise direction for both cases with and without heat transfer. These values are mass averaged on sections normal to the meridional direction. Point 1 is on the blade leading edge while point 2 is the on the blade trailing edge. The amount of work done on the flow can be calculated as follows:

$$w = \int_1^2 v\,dp = \int_1^2 \frac{dp}{\rho} \tag{17}$$

Fig. 7 illustrates P-V diagram for the compression process of two cases with and without internal heat transfer. The area between p-axis and diagrams shows the work input. Density is lower for the case with internal heat leakage due to the higher temperature of the flow. At the end of compression the pressure should be smaller for the case with internal heat leakage to keep the surrounded area which means work input was the same for both cases. Thus, the heat transfer to the impeller through the solid parts of the compressor from the hot region degrades the compression process.

The pressure ratio drop for different pressure ratios is shown in Fig. 8. The pressure drop due to internal heat transfer is small until pressure ratio of 4. After pressure ratio of 5 pressure drop increases rapidly. Increasing the rotational speed increases the pressure ratio and temperature ratio. The relationship between pressure ratio and temperature ratio is shown in Fig. 9. The increase rate in temperature ratio is high until pressure ratio of 4 and after that this increase becomes smaller. This leads to rapid increase in internal heat transfer under a pressure ratio of about 4.

After pressure ratio of 5 the pressure ratio drop increases dramatically. This seems to happen because of high Reynolds number in small radius part of the passage and the intensified Nusselt number. In the beginning of the passage the radius is small and only very high rotational speed increases the velocity of the flow near the shroud so that the Reynolds number reaches the critical value. The pressure ratio drop due to internal heat transfer can be neglected for pressure ratios lower than 5. The maximum decrease in the pressure ratio is about 0.83 at pressure ratio of about 11.

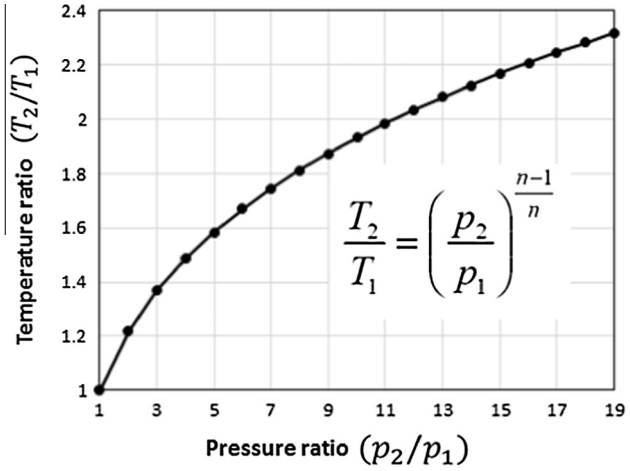

Fig. 9. Temperature ratio variation versus pressure ratio of the compressor.

3.2. Effects of the internal heat transfer on the efficiency

The compressor efficiencies with and without internal heat transfer are shown in Fig. 10. In this figure the black line is the pressure ratio of the compressor without including any solid part while the red line is the case with solid casing and solid impeller. The compressor efficiency decreases when the internal heat transfer is included. The efficiency drop increases with increasing pressure ratio.

As shown in Fig. 11, the entropy of the flow is higher when the internal heat transfer is present. The higher entropy of the flow then reduces the efficiency and this increases the work required for the same pressure rise. In addition, most of entropy rise due to the internal heat transfer happens in the tip clearance from the beginning of the main blade to about 80 percent of the blades length along the streamwise direction.

Fig. 12 shows a control volume encompassing the entire air flow region with δq as a small quantity of heat leaving at the higher temperature of T_2 and entering at the lower temperature of T_1. The entropy generation due to this heat transfer can be calculated as follows:

$$s_{gen} = \sum \delta q \left(\frac{1}{T_1} - \frac{1}{T_2}\right) \tag{18}$$

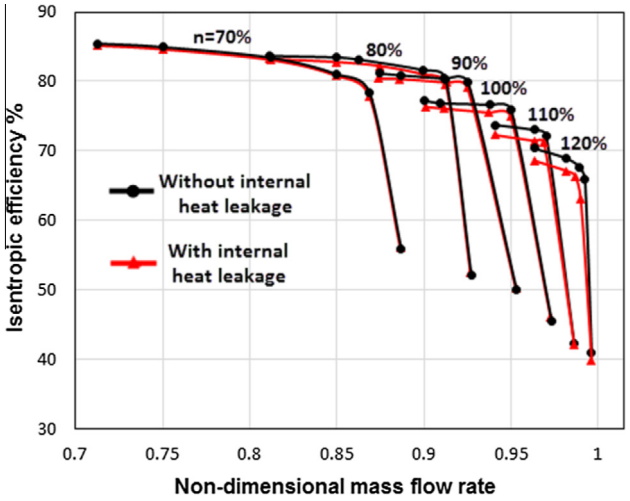

Fig. 10. Effect of internal heat leakage on the efficiency.

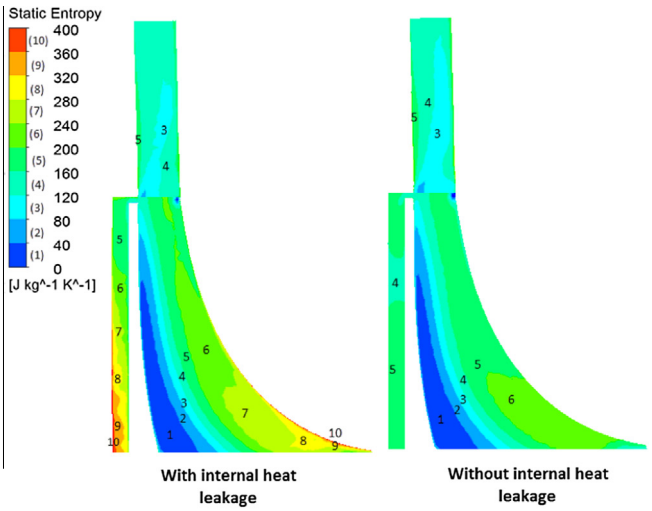

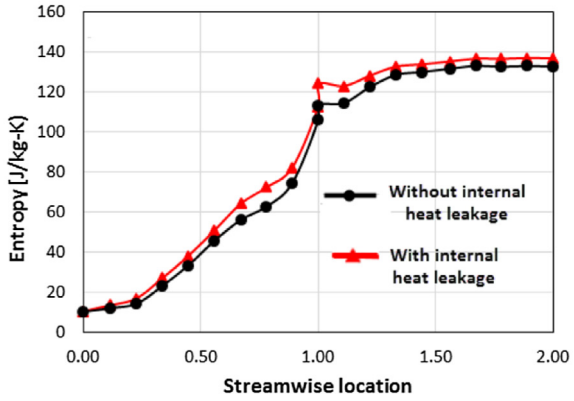

Fig. 11. Entropy inside the compressor with and without internal heat leakage.

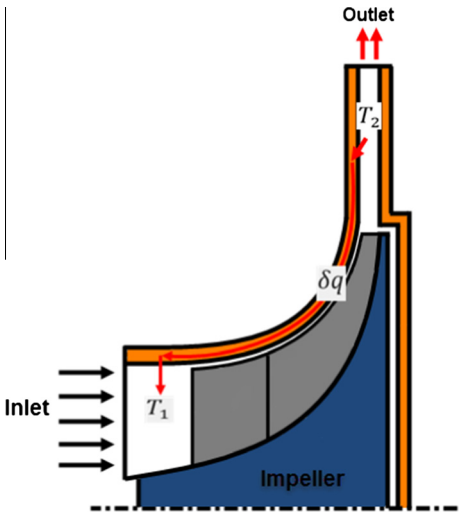

Fig. 12. Heat leakage path from the diffuser to the impeller.

where s_{gen} is the entropy generation due to the heat leakage. Increasing the average temperature difference between the hot and cool regions will increase the entropy generation. Also, non-uniform heat transfer will influence the flow streamlines which will lead to higher flow irreversibilities as explained by Greitzer [19]. The difference between the entropy changes in the compressor with and without internal heat is as follows:

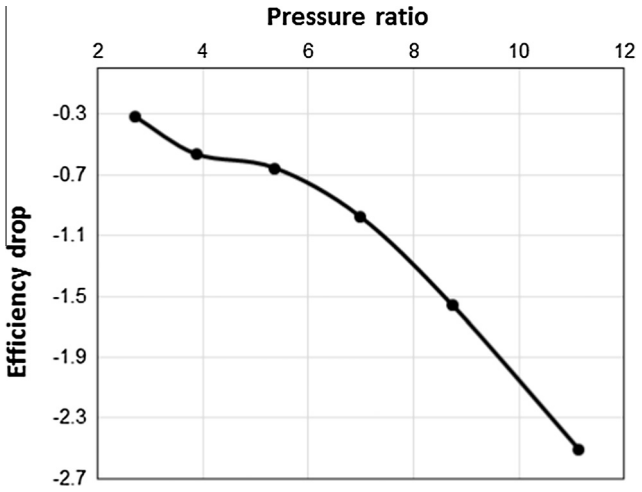

Fig. 13. Efficiency drop due to the internal heat leakage at different pressure ratios.

$$\Delta S = \Delta S_{gen} + \Delta S_{irr} = \sum \delta q \left(\frac{1}{T_1} - \frac{1}{T_2} \right) + \Delta S_{irr} \tag{19}$$

where ΔS_{irr} is the entropy rise due to increase in the flow irreversibilities. Higher flow irreversibilities and the entropy generation inside the compressor due to the internal heat leakage increase the flow enthalpy in the compressor with internal heat transfer.

The effect of the internal heat leakage on the efficiency for different pressure ratios is shown in Fig. 13. First efficiency drop increases with increasing the pressure ratio until pressure ratio of 4. Then the efficiency drop stays almost constant till pressure ratio of 5. After pressure ratio of 5 the efficiency drop increases exponentially with increasing pressure ratio due to the higher heat transfer rates with the higher temperature differences at higher pressure ratios. The maximum difference between the compressor efficiency with and without internal heat transfer is about 2.5% at pressure ratio around 11. This high efficiency drop at high pressure ratio highlights the important role that the internal heat transfer plays on the performance of a compact centrifugal compressor with high pressure ratio.

3.3. Effects of the solid impeller and solid casing

The effect of heat transfer through the solid casing and the solid impeller on the maximum impeller temperature will be investigated in this part. Different cases listed in Table 2 have been studied to understand the effect of heat leakage in different solid parts on the compressor efficiency and the impeller temperature. The maximum impeller temperatures are shown in Fig. 14 and the compressor isentropic efficiencies are shown in Fig. 15.

Fig. 15 shows that the compressor without any solid parts has the highest isentropic efficiency in comparison with the compressors with just the solid impeller or with both the solid impeller and the solid casing. The casing has an important effect in degrading the efficiency. The reason is the high amount of heat leakage from the diffuser to the middle of the impeller through the solid casing. Thus, the casing should be made of a low thermal conductivity material to reduce the heat leakage. However, as shown in Fig. 16 the heat transfer in the casing has little effect on the impeller temperature because the air gap temperature is already quite high due to the viscous heating. This reduces the temperature difference between diffuser and the backplate in the solid part and reduces the heat transfer.

Heat transfer inside the impeller is crucial for controlling the impeller temperature as demonstrated in Fig. 14. Meanwhile,

Table 2
Different solid region conditions.

Cases	Specification
Case 1	Solid casing and solid impeller
Case 2	No solid casing with just a solid impeller
Case 3	No solid casing and no solid impeller

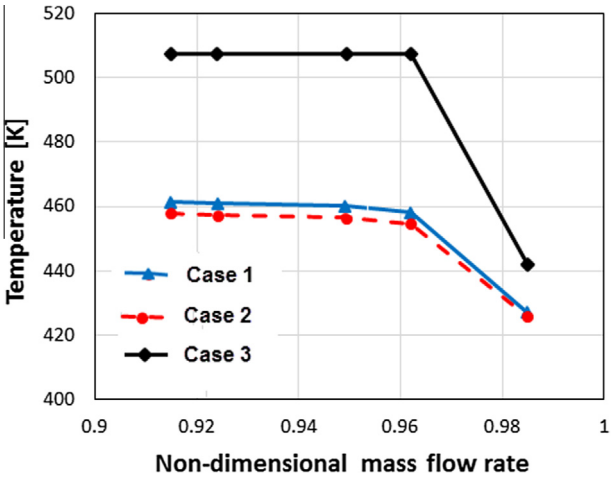

Fig. 14. Maximum impeller temperatures at 100% speed.

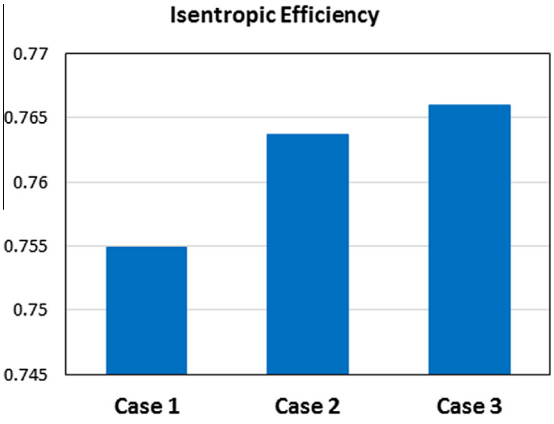

Fig. 15. Isentropic efficiencies for the three solid region cases listed in Table 2.

Fig. 15 shows that the heat transfer inside the impeller has relatively small influence on the efficiency. The solid impeller temperature increases in upstream while at the same time it decreases in downstream due to the heat leakage. Heat transfer to the air flow from the solid in upstream increases due to higher temperature of the solid impeller in this part. This heat transfer has a negative effect on the compression process and reduces the efficiency. However, because of lower temperature of the solid impeller in downstream there is a heat transfer back to the solid impeller from the air flow which increases the efficiency of the compression process. Though, the overall negative effect of heat leakage inside the impeller is small.

4. Conclusions

This study analyzed the effects of internal heat leakage through the solid parts from the hot downstream to the cool upstream on the compressor performance and reliability. A three dimensional CFD model was used to calculate the compressor performance

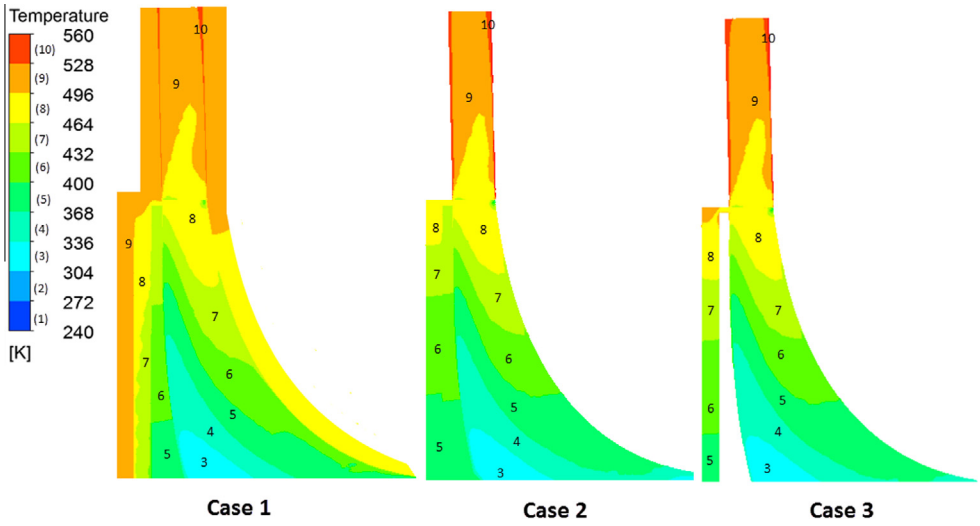

Fig. 16. Temperature profiles in the compressor for the three solid region cases listed in Table 2.

and the impeller temperature. The internal heat transfer in the solid parts was calculated using the CHT method. The results show that:

(1) The internal heat leakage reduces the maximum pressure ratio of the compressor. However, for pressure ratios less than 5 the internal heat transfer has little effect on the pressure ratio and can be neglected. For pressure ratios higher than 5, the effect of the internal heat transfer should be considered. The internal heat transfer reduces the pressure ratio by about 0.83 around pressure ratio of 11.
(2) The internal heat transfer reduces the compressor efficiency. The effect of the internal heat transfer on the efficiency deterioration increases exponentially with increasing pressure ratio. For pressure ratios higher than 5, the effect of the heat transfer on the efficiency has to be considered. The efficiency is reduced by 2.5% at pressure ratio up to 11 due to internal heat transfer.
(3) The internal heat transfer inside the impeller has a remarkable effect on the impeller temperature and effectively reduces the maximum impeller temperature. Conventional simulations often neglect this heat transfer and then overpredict the maximum impeller temperature. The solid casing has little effect of the impeller temperature. The effect of the internal heat transfer inside the solid impeller on the maximum impeller temperature must be considered when developing high pressure ratio compressors (with pressure ratios more than 5).

Acknowledgements

This research was supported by the National Natural Science Foundation of China (Grant No. 51176087).

References

[1] H. Krain, B. Hoffmann, et al., Improved high pressure ratio centrifugal compressor, ASME, Paper No. GT2007-27100, 2007, pp. 967–975.
[2] H. Krain, B. Hoffmann, Flow study of a redesign high-pressure ratio centrifugal compressor, ASME Paper No. GT2010-23714, 2010, pp. 1027–1040.
[3] M. Oana, H. Ohtani, Approach to high performance transonic compressor design, J. Propul. Power 20 (1) (2004).
[4] C. Zhang, Q. Deng, Study on aerodynamic redesign of high pressure ratio centrifugal compressor, ASME, Paper No. GT2010-23714, 2010, pp. 1027–1040.
[5] A. Romagnoli, R. Martinez-Botas, Heat transfer on a turbocharger under constant load points, ASME paper No. GT2009-59618, 2009.
[6] X.Q. Zheng, L. Jin, Effect of temperature on the strength of a centrifugal compressor impeller for a turbocharger, Part C - J. Mech. Eng. (2013).
[7] T. Gwehenberger, M. Thiele, M. Seiler, et al., Single-stage high-pressure turbocharging, ASME Paper No. GT2009-59322, 2009.
[8] S.M. Moosania, X.Q. Zheng, Performance improvement of a high pressure ratio centrifugal compressor by integrated cooling, Proc. IMechE Part G: J. Aerosp. Eng. (2015) 1–8.
[9] L.L. Gu, Numerical study of the heat transfer effect on a centrifugal compressor performance, Proc. IMech Eng. Sci. (2014) 1–14.
[10] M. Cui, Numerical and experimental investigation of heat transfer in a low flow single stage centrifugal compressor, ASME GT2016-57710, 2016.
[11] Y. Jaluria, Computational Heat Transfer, vol. 21, CRC Press, 2002, November.
[12] M.P. Bulat, P.V. Bulat, Comparison of turbulence models in the calculation of supersonic separated flow, World Appl. Sci. 27 (1) (2013) 1263–1266.
[13] G. Lin, Conjugate heat transfer analysis of convection-cooled turbine vanes using γ-$Re\theta$ transition model, Int. J. Gas Turbine Propul. Power Syst. 6 (3) (2014) 9–15.
[14] P.R. Spalart, M. Shur, On the sensitization of turbulence models to rotation and curvature, Aerosp. Sci. Technol. 1 (5) (1997) 297–302.
[15] T.J. Barth, D.C. Jesperson, The design and application of upwind schemes on unstructured meshes, AIAA paper 89-0366.
[16] V. Tom, R.V. Braembussche, A novel method for the computation of conjugate heat transfer with coupled solvers, in: Int. Symp. on Heat Transfer in Gas Turbine Systems, 2009.
[17] E. Divo, E. Steinthorsson, Conjugate heat transfer solver for large scale turbomachinery models, NASA report CR 212195, 2003.
[18] H. Krain, B. Hofmann, Aerodynamic of a Centrifugal Compressor Impeller with Transonic Inlet Conditions, ASME, 1995.
[19] E. Greitzer, Internal Flow Concepts and Applications, Cambridge University Press, 2007.